THE JOURNAL OF BIOLOGICAL CHEMISTRY VOL. 291, NO. 31, pp. 16249–16262, July 29, 2016


# Exon Skipping in the *RET* Gene Encodes Novel Isoforms That Differentially Regulate RET Protein Signal Transduction*

Received for publication, December 11, 2015, and in revised form, May 9, 2016 Published, JBC Papers in Press, May 23, 2016, DOI 10.1074/jbc.M115.709675

**Nicole A. Gabreski[‡§], Janki K. Vaghasia[‡], Silvia S. Novakova[‡], Neil Q. McDonald[¶‖], and Brian A. Pierchala[‡§1]**

*From the [‡]Department of Biologic and Materials Sciences, University of Michigan School of Dentistry, Ann Arbor, Michigan 48109, the [§]Program in Cellular and Molecular Biology, University of Michigan School of Medicine, Ann Arbor, Michigan 48109, the [¶]Structural Biology Laboratory, Francis Crick Institute, 44 Lincoln's Inn Fields, London WC2A 3LY, United Kingdom, and the [‖]Institute of Structural and Molecular Biology, Department of Biological Sciences, Birkbeck College, Malet Street, London WC1E 7HX, United Kingdom*

**Rearranged during transfection (RET), a receptor tyrosine kinase that is activated by the glial cell line-derived neurotrophic factor family ligands (GFLs), plays a crucial role in the development and function of the nervous system and additionally is required for kidney development and spermatogenesis. *RET* encodes a transmembrane receptor that is 20 exons long and produces two known protein isoforms differing in C-terminal amino acid composition, referred to as RET9 and RET51. Studies of human pheochromocytomas identified two additional novel transcripts involving the skipping of exon 3 or exons 3, 4, and 5 and are referred to as $RET^{\Delta E3}$ and $RET^{\Delta E345}$, respectively. Here we report the presence of $Ret^{\Delta E3}$ and $Ret^{\Delta E345}$ in zebrafish, mice, and rats and show that these transcripts are dynamically expressed throughout development of the CNS, peripheral nervous system, and kidneys. We further explore the biochemical properties of these isoforms, demonstrating that, like full-length RET, $RET^{\Delta E3}$ and $RET^{\Delta E345}$ are trafficked to the cell surface, interact with all four GFRα co-receptors, and have the ability to heterodimerize with full-length RET. Signaling experiments indicate that $RET^{\Delta E3}$ is phosphorylated in a similar manner to full-length RET. $RET^{\Delta E345}$, in contrast, displays higher baseline autophosphorylation, specifically on the catalytic tyrosine, $Tyr^{905}$, and also on one of the most important signaling residues, $Tyr^{1062}$. These data provide the first evidence for a physiologic role of these isoforms in RET pathway function.**

RET is a receptor tyrosine kinase that is critical for kidney morphogenesis, spermatogenesis, and development of the nervous system (1–4). RET is activated by a family of four growth factors known as the glial cell line-derived neurotrophic factor (GDNF)[2] family ligands (GFLs), which includes GDNF, neurturin, artemin, and persephin (1). Each GFL binds to one of four cognate glycosylphosphatidylinositol-anchored co-receptors known as the GDNF family receptor αs (GFRαs) (2, 5). The GFL-GFRα complex binds to RET, inducing RET dimerization and subsequent autophosphorylation on multiple tyrosine residues within the intracellular tyrosine kinase domain. This enhances tyrosine kinase activity and initiates the association of adaptor proteins and enzymes that trigger multiple second messenger cascades (6).

The presence of two major Ret isoforms, RET9 and RET51, has been extensively described in the literature, and a third isoform, RET43, has also been observed in humans (7–9). *Ret* is 20 exons long, and *Ret9* and *Ret51* transcripts differ in alternative splicing of intron 19. Intron 19 in the *Ret51* transcript is excised properly, whereas, in the *Ret9* transcript, the intron is retained, changing the reading frame and inserting a premature stop codon into the amino acid sequence. This creates a unique nine-amino acid C-terminal sequence for RET9 and a unique 51-amino acid C-terminal sequence for RET51. Interestingly, these two different isoforms display marked differences in their degradation and function (7, 10, 11).

Three additional *Ret* transcripts have been reported in various tumor sources as well as adult human tissues (12). These novel transcripts are a product of exon skipping in the 5′ region of *RET*, which encodes for the extracellular domain of the protein. Skipping of exons 3 ($RET^{\Delta E3}$) or exons 3, 4 and 5 ($RET^{\Delta E345}$) gives rise to transcripts that encode for full-length Ret proteins but with deletions in the extracellular domain, specifically cadherin-like domain 1 (CLD1) or CLD1–3, respectively. These deletions are hypothesized to change the extracellular domain structure as well as binding to GFL-GFRα complexes and may impact the overall stability of the proteins. The skipping of exons 3 and 4 results in a frameshift that culminates in a premature stop. This protein encodes only a small portion of the RET extracellular domain with no transmembrane or intracellular domain. Because this transcript is likely to be subjected to nonsense-mediated decay, it is unlikely to be involved in RET signal transduction.

* This work was supported by National Institutes of Health Grant R01 NS089585 (to B. A. P.). Additional funding support came from the University of Michigan Cellular and Molecular Biology Predoctoral Fellowship T32-GM007315 (to N. A. G.). The authors declare that they have no conflicts of interest with the contents of this article. The content is solely the responsibility of the authors and does not necessarily represent the official views of the National Institutes of Health.

[1] To whom correspondence should be addressed: Dept. of Biologic and Materials Sciences, University of Michigan School of Dentistry, 1011 N. University Ave., Ann Arbor, MI 48109. Tel.: 734-763-3394; Fax: 734-647-2110; E-mail: pierchal@umich.edu.

[2] The abbreviations used are: GDNF, glial cell line-derived neurotrophic factor; GFL, glial cell line-derived neurotrophic factor family ligand; GFR, glial cell line-derived neurotrophic factor family receptor; MEN, multiple endocrine neoplasia; E19.5, embryonic day 19.5; CLD, cadherin-like domain; DRG, dorsal root ganglion/ganglia; SCG, superior cervical ganglion/ganglia; qPCR, quantitative PCR; P3, postnatal day 3; RET, rearranged during transfection; IRES, internal ribosome entry site.

Here we show that $Ret^{\Delta E3}$ and $Ret^{\Delta E345}$ transcripts are conserved in vertebrates and that the mRNA and proteins of these splice variants are expressed throughout the nervous system in mice. We also show that these isoforms are trafficked to the cell surface and that both isoforms interact with all four GFRαs. Additionally, we find that $RET^{\Delta E3}$ is phosphorylated to a similar level as full-length RET and is activated in a GDNF-dependent manner. However, $RET^{\Delta E345}$ displays higher baseline autophosphorylation, specifically on the catalytic tyrosine $Tyr^{905}$, and also on an additional signaling tyrosine, $Tyr^{1062}$. Interestingly, $RET^{\Delta E345}$ is not activated in a GDNF-dependent manner. Taken together, these isoforms may have unique and important unidentified roles in the development and maintenance of the nervous system and kidneys as well as in the pathophysiology of neuroendocrine gland diseases.

## Results

*Exons 3, 4, and 5 of Ret Are Not Highly Conserved, but $Ret^{\Delta E3}$ and $Ret^{\Delta E345}$ Transcripts Are Observed in Several Organisms*—It has been described previously that the intracellular domain of RET, which contains a tyrosine kinase domain, is more highly conserved than the extracellular domain (13). To better understand the level of conservation of amino acids encoded by each exon, we compared sequences from zebrafish (*Danio rerio*), mouse (*Mus musculus*), rat (*Rattus norvegicus*), and human (*Homo sapiens*). We found that the entire intracellular domain was more than 75% conserved at the amino acid level. This was not surprising because mutations in many of these highly conserved regions give rise to loss of function (*e.g.* Hirschsprung disease) or gain of function (*e.g.* multiple endocrine neoplasia type 2A (MEN2A) and 2B (MEN2B)) phenotypes (Fig. 1*A*). Interestingly, exons 3, 4, and 5 are less than 50% conserved between these species. Although this lack of conservation is suggestive that these regions of RET are not as functionally important, it could also be interpreted as allowing for amino acid flexibility between the different RET isoforms.

Our initial sequence analysis suggested that $Ret^{\Delta E3}$ and $Ret^{\Delta E345}$ transcripts could be expressed in additional vertebrates other than *H. sapiens*. These transcripts were originally identified in human kidney and substantia nigra fetal tissues (12). Sequence analysis demonstrated that exon skipping also encodes potential full-length transcripts in zebrafish, mice, and rats (Fig. 1*A*). To determine whether these novel transcripts were expressed in these organisms, species-specific primers were created to identify each of the *Ret* transcripts: full-length *Ret*, $Ret^{\Delta E3}$, and $Ret^{\Delta E345}$. RT-PCR analysis identified the presence of $Ret^{\Delta E3}$ and $Ret^{\Delta E345}$ from 48 hours post fertilization zebrafish embryos, E19.5 rat dorsal root ganglia, and E18.5 mouse spinal cord (Fig. 1*B*). Sequence analysis confirmed these amplicons to be $Ret^{\Delta E3}$ and $Ret^{\Delta E345}$ (data not shown). This is the first time these transcripts have been identified in vertebrates other than *H. sapiens*. Taken together, these data indicate that 5′ exon skipping is conserved and results in the expression of $Ret^{\Delta E3}$ and $Ret^{\Delta E345}$ transcripts.

*Exon Skipping Creates Large Deletions in the Extracellular Domain of RET*—To understand the impact deletions in the extracellular domain would have on RET, we analyzed the deletions in terms of a CLD1–4 model derived from electron microscopy and small angle x-ray scattering analyses (14). The main consequence of deletion of exon 3 is the removal of half of CLD1 (residues 113–150) and half of CLD2 (residues 154–208). Each domain adopts a β sandwich cadherin fold comprised of two β sheets separated by numerous buried hydrophobic residues. Elimination of exon 3 removes one sheet from CLD1 and several β strands from both sheets of CLD2 (Fig. 1*C*). Therefore, it is likely that both CLD domains are substantially perturbed leaving β strands without the cadherin fold structure and exposing some hydrophobic residues. Exon 3 removal also eliminates a highly constrained Cis-Pro loop ($Cys^{137}$-$Cys^{142}$) unique to higher vertebrate RET sequences. The portion of CLD1–2 removed coincides with regions stabilizing the clam shell arrangement of CLD1–2 (15). This would result in a more open and extended arrangement for the remaining parts of CLD1 and CLD2 with much greater flexibility between the domains. An odd number of cysteine residues (three in total) are deleted by removing exon 3, including the $Cys^{157}$-$Cys^{197}$ disulfide. $Cys^{166}$ is also removed, leaving its partner $Cys^{243}$ unpaired but buried. The two unpaired cysteines, $Cys^{87}$ and $Cys^{216}$, which constitute a known folding bottleneck in wild-type RET, are left untouched. We expect $RET^{\Delta E3}$ to be a less stable transmembrane protein with a short half-life that retains at least some ligand-binding properties.

For $RET^{\Delta E345}$, removal of exons 3, 4, and 5 effectively eliminates much of CLD1–3 but leaves CLD4-cysteine-rich domain (CRD) intact (Fig. 1*C*). This region by itself was shown to be insufficient to bind ligand but retains at least one important binding epitope (*i.e.* necessary for ligand binding but not sufficient) (14). Many receptor tyrosine kinases have extracellular domains that have autoinhibitory functions in the absence of ligand. Deletion of such regions can lead to autoactivation in a ligand-independent manner. By analogy with these other systems, removal of CLD1–3 could leave a truncated form of RET that would be constitutively activated in the absence of ligand and likely would be unresponsive to the GFLs.

*$Ret^{\Delta E3}$ and $Ret^{\Delta E345}$ Are Co-expressed in Several Tissues with Ret throughout Development*—To determine where and when $Ret^{\Delta E3}$ and $Ret^{\Delta E345}$ transcripts are expressed and whether their expression levels change over time, we analyzed tissues in which full-length *Ret* is expressed at several developmental time points. Within the central nervous system, we analyzed the brain, as signaling via Ret is important for the survival of central noradrenergic neurons and dopaminergic neurons in the ventral midbrain, as well as the spinal cord, where GDNF/GFRα1/Ret signaling is critical for axon guidance into the hind limbs and survival of γ motor neurons (16–21). In the peripheral nervous system, we analyzed sensory neurons of the dorsal root ganglia (DRG), where neurturin/GFRα2/Ret signaling is important for the survival and maintenance of mechanoreceptors during development (22, 23). Additionally, shortly after birth, a subclass of nociceptors transition from being TrkA-positive to expressing GFRα1/Ret to support the development and survival of nonpeptidergic nociceptors (24–26). Sympathetic neurons of the superior cervical ganglia (SCG) were also analyzed, as it has been well established that artemin/GFRα3/Ret signaling is necessary for proper sympathetic chain migra-

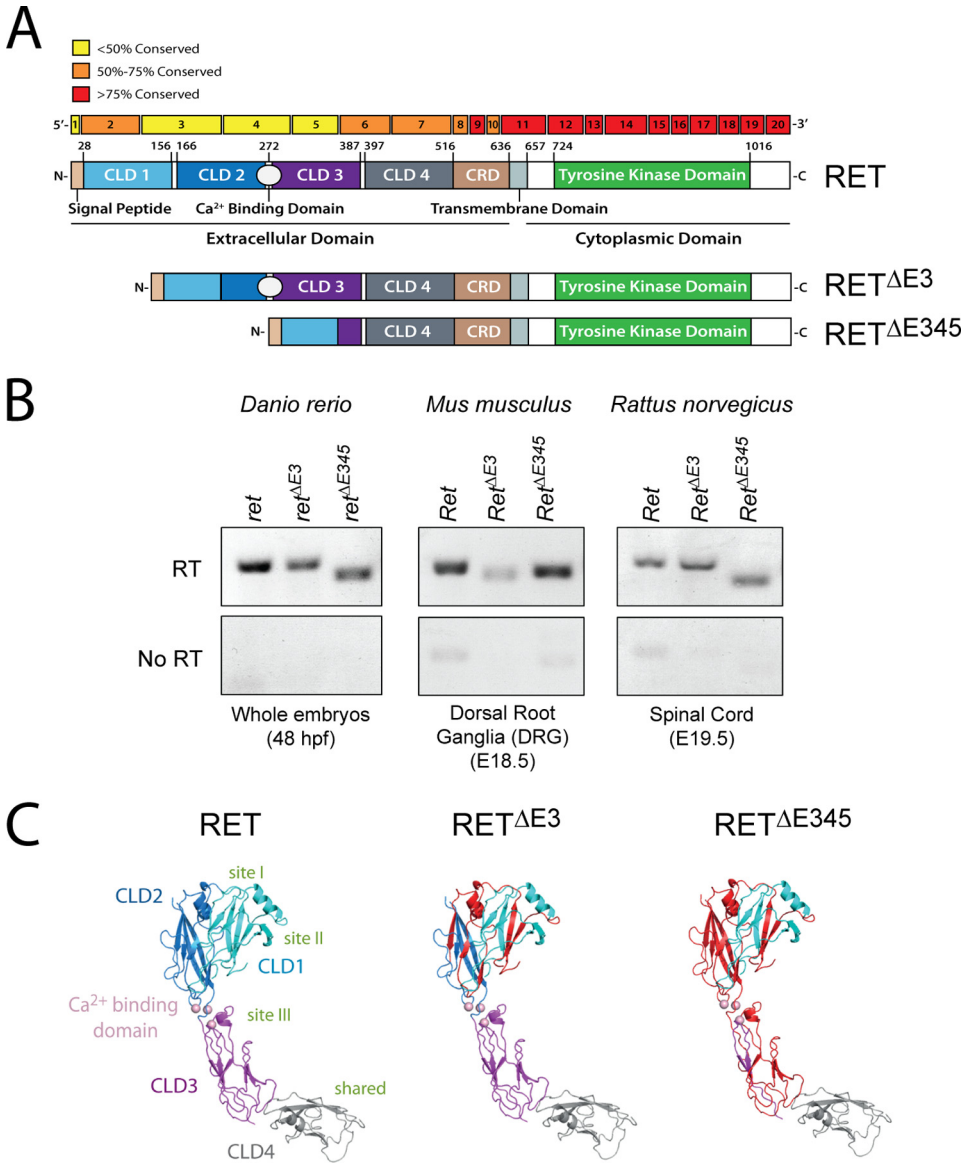


FIGURE 1. **Removal of exons 3 or 3, 4, and 5 of *RET* creates proteins with large deletions in the extracellular domain, and transcripts encoding these receptors are expressed in multiple organisms.** *A*, comparison of the amino acid sequences of RET between zebrafish, mice, rats, and humans was performed, and the conservation within each exon is indicated by color. Interestingly, the amino acids encoded in exons 3, 4, and 5 are the least conserved. Additionally, the impact of exon skipping on the extracellular domain within the protein is shown. *B*, $Ret^{\Delta E3}$ and $Ret^{\Delta E345}$ transcripts are detectable in zebrafish (*D. rerio*), mice (*M. musculus*), and rats (*R. norvegicus*) by qPCR. Like human $RET^{\Delta E3}$ and $RET^{\Delta E345}$, alternative splicing of exon 3 or exons 3, 4, and 5 in these vertebrates are predicted to encode full-length, transmembrane RET proteins with deletions in the extracellular domain. *C*, deleted regions are shown in *red*, projected onto a structural model for RET cadherin domains 1–4 derived from PDB code 4UX8.

tion and axon guidance during development (27–29). Last, the kidney was analyzed because GDNF/GFRα1/Ret signaling is crucial for ureteric bud branching and morphogenesis of the kidney (30–34). Using qPCR, we examined the relative expression of *Ret*, $Ret^{\Delta E3}$, and $Ret^{\Delta E345}$ in each of these tissues in mice and found that they were detected in all five tissues. The relative expression of *Ret*, $Ret^{\Delta E3}$, and $Ret^{\Delta E345}$ was lower in the brain, spinal cord, and kidney (Fig. 2*A*) compared with the DRG and SCG (Fig. 2*B*). Interestingly, in the spinal cord, DRG, and SCG, there was a significant increase of $Ret^{\Delta E3}$ expression at E19.5 that preceded a significant increase of *Ret* at P3. The expression of all three transcripts was highest in the DRG, particularly at E19.5 and P3, when the IB4+ subpopulation of nociceptors is emerging.

*5′ and 3′ Alternative Splicing of Ret transcripts Are Not Mutually Exclusive*—Alternative splicing of intron 19 in *Ret* allows for the translation of two isoforms of Ret, RET9 and RET51. We sought to determine whether alternative splicing could occur simultaneously, both 5′ and 3′ in *Ret* transcripts, allowing for increased diversity of encoded RET proteins. cDNA was isolated from E19.5 mouse DRGs, as we found this tissue to have the highest relative expression of *Ret*, $Ret^{\Delta E3}$, and $Ret^{\Delta E345}$ (Fig. 2*B*). Forward primers specific for each 5′ splicing event were paired with reverse primers that would detect either *Ret9* or *Ret51* alternative splicing. Full-length *Ret9* and *Ret51* transcripts were detected, as expected, at 3.33 kb and 4.38 kb, respectively. We observed $Ret^{\Delta E3}$ and $Ret^{\Delta E345}$ with intron 19 retention, thus encoding $Ret^{\Delta E3}$ and $Ret^{\Delta E345}$ transcripts with

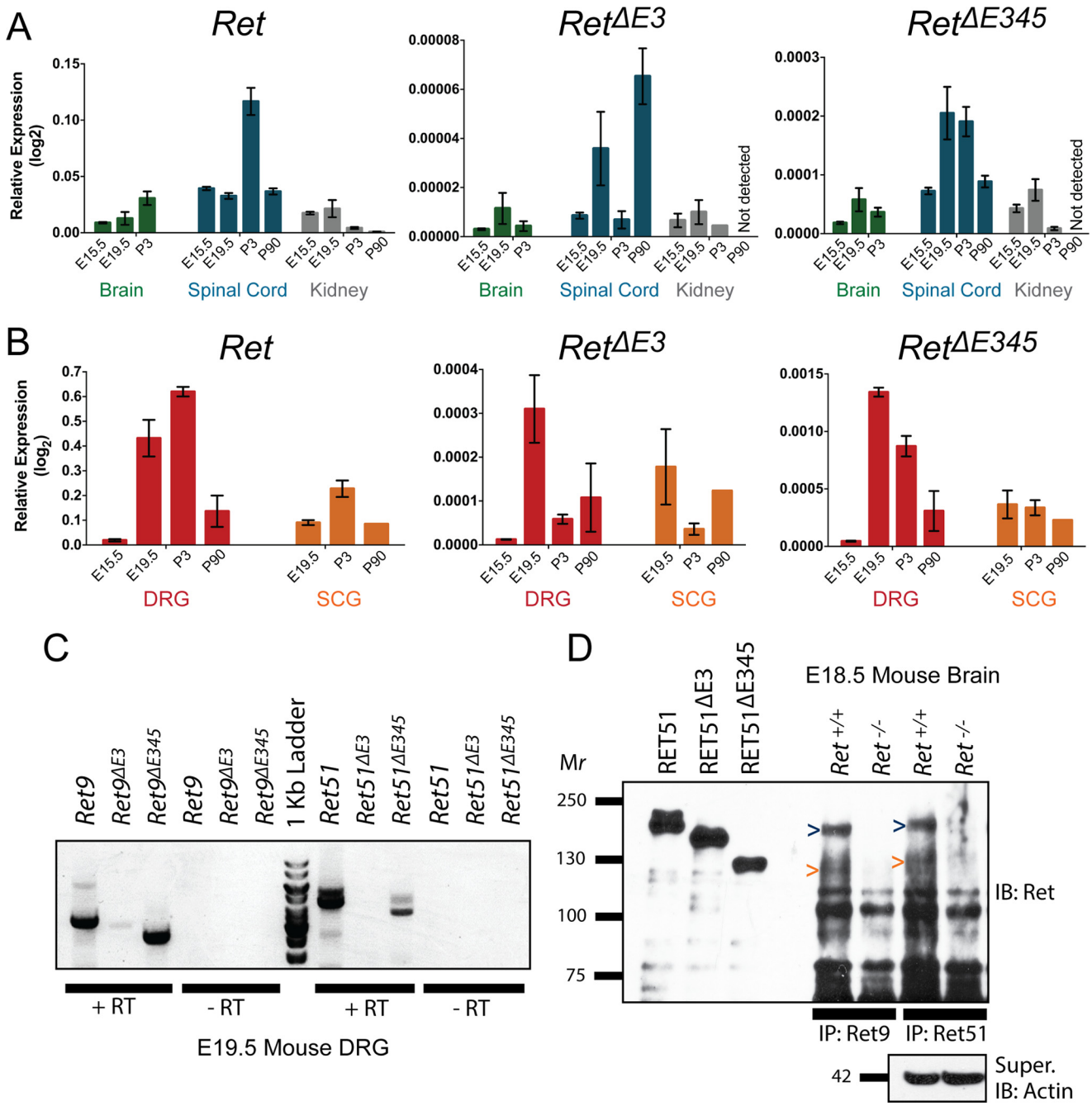


FIGURE 2. ***Ret*$^{\Delta E3}$ and *Ret*$^{\Delta E345}$ are dynamically expressed throughout development, and RET proteins with similar molecular weights as RET$^{\Delta E345}$ are detect *in vivo*.** *A*, expression of *Ret*, *Ret*$^{\Delta E3}$, and *Ret*$^{\Delta E345}$ in mouse brain (*E15.5*, *E19.5*, *P3*), spinal cord (*E15.5*, *E19.5*, *P3*, *adult*), and kidney (*E15.5*, *E19.5*, *P3*, *adult*) by qPCR is shown as relative expression compared with *actin*. *B*, expression of *Ret*, *Ret*$^{\Delta E3}$, and *Ret*$^{\Delta E345}$ in mouse sympathetic (*E19.5*, *P3*, *adult*) and DRG sensory neurons (*E15.5*, *E19.5*, *P3*, *adult*) by qPCR is graphed as in *A*. *C*, cDNA from E19.5 DRGs was synthesized from poly(A) RNA, and RT-PCR was performed to determine the presence of *Ret* transcripts with both 5′ and 3′ alternative splicing. *Ret9*, *Ret9*$^{\Delta E3}$, *Ret9*$^{\Delta E345}$, *Ret51*, and Ret51$^{\Delta E345}$ transcripts were identified. *D*, E18.5 mouse brains were lysed, and immunoprecipitations (*IP*) for RET9 or RET51 were performed. Immunoblotting for RET detected full-length RET9 and RET51, as expected. The presence of RET9 and RET51 proteins at the same molecular weight as RET$^{\Delta E345}$ suggested the existence of RET9$^{\Delta E345}$ and RET51$^{\Delta E345}$ isoforms.

amplicons of 3.05 kb and 2.61 kb, respectively. However, we were only able to detect *Ret*$^{\Delta E345}$ with a properly excised intron 19 at an amplicon size of 3.66 kb, encoding a *Ret51*$^{\Delta E345}$ transcript. Although we were unable to detect a *Ret51*$^{\Delta E3}$ transcript (4.10 kb), this is likely due to the generally low expression levels of *Ret*$^{\Delta E3}$. Taken together, these data indicate that the *Ret* locus encodes for at least three previously unidentified transcripts and at least five total Ret isoforms: *Ret9*, *Ret9*$^{\Delta E3}$, *Ret9*$^{\Delta E345}$, *Ret51*, and *Ret51*$^{\Delta E345}$.

*RET Proteins of the Same Molecular Weight as RET*$^{\Delta E345}$ *Are Detected in Vivo*—Although we can detect *Ret*$^{\Delta E3}$ and *Ret*$^{\Delta E345}$ mRNA transcripts, which are likely being processed for translation, we sought to detect the presence of these isoforms at the protein level. Plasmids encoding human *RET51*, *RET51*$^{\Delta E3}$, and *RET51*$^{\Delta E345}$ were transfected into NIH/3T3 cells, and lysates were run as size standards to aid in detecting Ret isoforms of the appropriate molecular weights from E18.5 mouse brain. The molecular weight of native RET51 protein is 120 kDa, but

because of posttranslational modifications, specifically glycosylation of the extracellular domain, RET51 has a molecular weight of ~180 kDa. The native molecular weights of $RET^{\Delta E3}$ and $RET^{\Delta E345}$ were predicted to be 109 kDa and 93 kDa, respectively. In transfected cells, we consistently observe the mature, processed proteins to have molecular weights of ~150 kDa ($RET^{\Delta E3}$) and ~125 kDa ($RET^{\Delta E345}$) (Fig. 2*D*).

Whole brains from $Ret^{+/+}$ or $Ret^{-/-}$ E18.5 littermate mice were lysed and divided in two, and immunoprecipitations were performed to isolate either RET9 or RET51 proteins. Although the qPCR data suggested that *Ret* transcripts have an overall lower relative expression in the brain compared with PNS tissues, the brain was chosen for analysis because of the abundant amount of protein that could be isolated. $Ret^{-/-}$ mice were used as a control to demonstrate the specificity of RET immunoblotting and to show the potential presence of RET proteins at the same molecular weight as $RET^{\Delta E3}$ and $RET^{\Delta E345}$. Because we previously observed more highly expressed $Ret9^{\Delta E345}$ and $Ret51^{\Delta E345}$ transcripts compared with those of $Ret^{\Delta E3}$, we hypothesized that we would be most able to detect both $RET9^{\Delta E345}$ and $RET51^{\Delta E345}$ proteins. By immunoblotting for RET, we were able to detect full-length RET9 and RET51 proteins, as expected (Fig. 2*D*). Additionally, we observed RET9 and RET51 bands with similar molecular weights to $RET^{\Delta E345}$, suggesting the presence of $RET9^{\Delta E345}$ and $RET51^{\Delta E345}$ proteins in mouse brain (Fig. 2*D*). Because the antibodies used for immunoprecipitations of RET9 and RET51 are to the C terminus, and the RET antibody for immunoblotting is to the common N-terminal region, this RET protein is unlikely to be a degradation product. However, we cannot exclude the possibility that this is an immature, non-glycosylated, full-length RET protein.

*$RET^{\Delta E3}$ and $RET^{\Delta E345}$ Are Trafficked to the Cell Surface*—To examine the biochemical properties of $RET^{\Delta E3}$ and $RET^{\Delta E345}$, we transitioned to an *in vitro* system for these experiments. Although $RET^{\Delta E3}$ and $RET^{\Delta E345}$ encode proteins that may be capable of signaling, this does not guarantee that they will be correctly trafficked to the cell surface for activation. To determine whether $RET^{\Delta E3}$ and $RET^{\Delta E345}$ are trafficked to the plasma membrane, NIH/3T3 cells were transfected with C-terminally epitope-tagged *Ret* constructs that also contain an IRES-GFP to serve as an indicator for transfected cells. Taking advantage of a RET antibody specific for the extracellular domain and using an HA antibody to label the C terminus of RET, we were able to selectively visualize RET located on the plasma membrane. Full-length RET was detected on the cell surface of transfected NIH/3T3 cells, as expected (Fig. 3*K*). Permeabilization revealed the C-terminal HA tag, confirming the integrity of the plasma membrane (Fig. 3*P*). Similar to full-length RET, both $RET^{\Delta E3}$ and $RET^{\Delta E345}$ were trafficked to the cell surface, as determined with the extracellular RET antibody in non-permeabilized cells (Fig. 3, *S* and *A'*). Transfection of GFP alone showed no labeling with the RET and HA antibodies, regardless of permeabilization, confirming the specificity of our immunostaining (Fig. 3, *A*–*H*). A cell surface biotinylation experiment was performed as a secondary measure to confirm these results, and we again observed trafficking of full-length RET, $RET^{\Delta E3}$, and $RET^{\Delta E345}$ to the cell surface (data not shown). Thus, $RET^{\Delta E3}$ and $RET^{\Delta E345}$ are trafficked properly to the cell surface, where they can participate in GFL-mediated activation.

*$RET^{\Delta E3}$ and $RET^{\Delta E345}$ Bind to GFRα1, GFRα2, GFRα3, and GFRα4*—Previous structural analysis (Fig. 1*C*) suggested that interactions between $RET^{\Delta E3}$ and the GFRαs may be unstable and that $RET^{\Delta E345}$ would be unlikely to bind to the co-receptors because of deletions of important binding residues in CLD1 and CLD3. To confirm these results, we co-transfected HEK293T cells with $RET^{\Delta E3}$ or $RET^{\Delta E345}$ and HA epitope-tagged *GFRα* constructs (*HA::GFRα1* (mouse), *HA::GFRα2* (rat), *HA::GFRα3* (mouse), and *HA::GFRα4* (chicken)). Immunoprecipitations were performed using a stringent immunoprecipitation buffer (modified radioimmune precipitation assay buffer) to eliminate any weak, nonspecific interactions. Surprisingly, we found that both $RET^{\Delta E3}$ and $RET^{\Delta E345}$ bind to each of the four GFRαs (Fig. 4). Co-transfection of the GFRαs with TrkA, another receptor tyrosine kinase, was performed as a negative control to show selectivity of binding between the GFRαs and RET (Fig. 4). As expected, TrkA did not associate with any of the GFRαs. There were no apparent differences between the four different GFRαs in regard to the extent of their association with $RET^{\Delta E3}$ and $RET^{\Delta E345}$, suggesting that these splice variants could potentially be activated by all four GFLs (Fig. 4).

*$RET^{\Delta E3}$ and $RET^{\Delta E345}$ Heterodimerize with Full-length RET*—In addition to being potential signaling molecules on their own, we observed that these transcripts are normally expressed in tissues where full-length RET is also expressed (Fig. 2). Although these isoforms may be present in different cells within these tissues, these observations raise the question of whether $RET^{\Delta E3}$ and $RET^{\Delta E345}$ could heterodimerize with full-length RET and affect its function. To test this possibility, HEK293T cells were co-transfected with HA epitope-tagged *RET51* and untagged $RET^{\Delta E3}$ or $RET^{\Delta E345}$. Immunoprecipitations were performed using an HA antibody to select for full-length RET51 and determine whether the different isoforms could interact with one another (Fig. 5*A*). In an additional experiment, FLAG-tagged $RET51^{\Delta E345}$ (FLAG:: $RET51^{\Delta E345}$) was co-transfected with *RET51* and $RET51^{\Delta E3}$, and immunoprecipitations were performed using a FLAG antibody to select for $RET51^{\Delta E345}$ (Fig. 5*B*). We found that both $RET51^{\Delta E3}$ and $RET51^{\Delta E345}$ associated with full-length RET51 and that $RET51^{\Delta E3}$ and $RET51^{\Delta E345}$ could also bind to one another (Fig. 5). This is consistent with former experiments suggesting that overexpression of RET proteins allows for ligand-independent dimerization via the transmembrane domain (35).

*$RET^{\Delta E345}$ Has Increased Ligand-independent Activation Compared with RET and $RET^{\Delta E3}$*—To determine levels of activation of $RET^{\Delta E3}$ and $RET^{\Delta E345}$, the basal phosphorylation of tyrosine residues of the RET isoforms were compared with full-length RET phosphorylation. Overexpression of the RET isoforms *in vitro*, either in the presence or absence of a GFRα, allows for ligand-independent dimerization and activation of RET. The level of activation can be assessed by determining the summated level of all of the phosphorylated tyrosines using a pan-phosphotyrosine antibody, or individual tyrosine residues can be analyzed using residue-specific RET phosphotyrosine antibodies. We evaluated the level of total phosphotyrosine

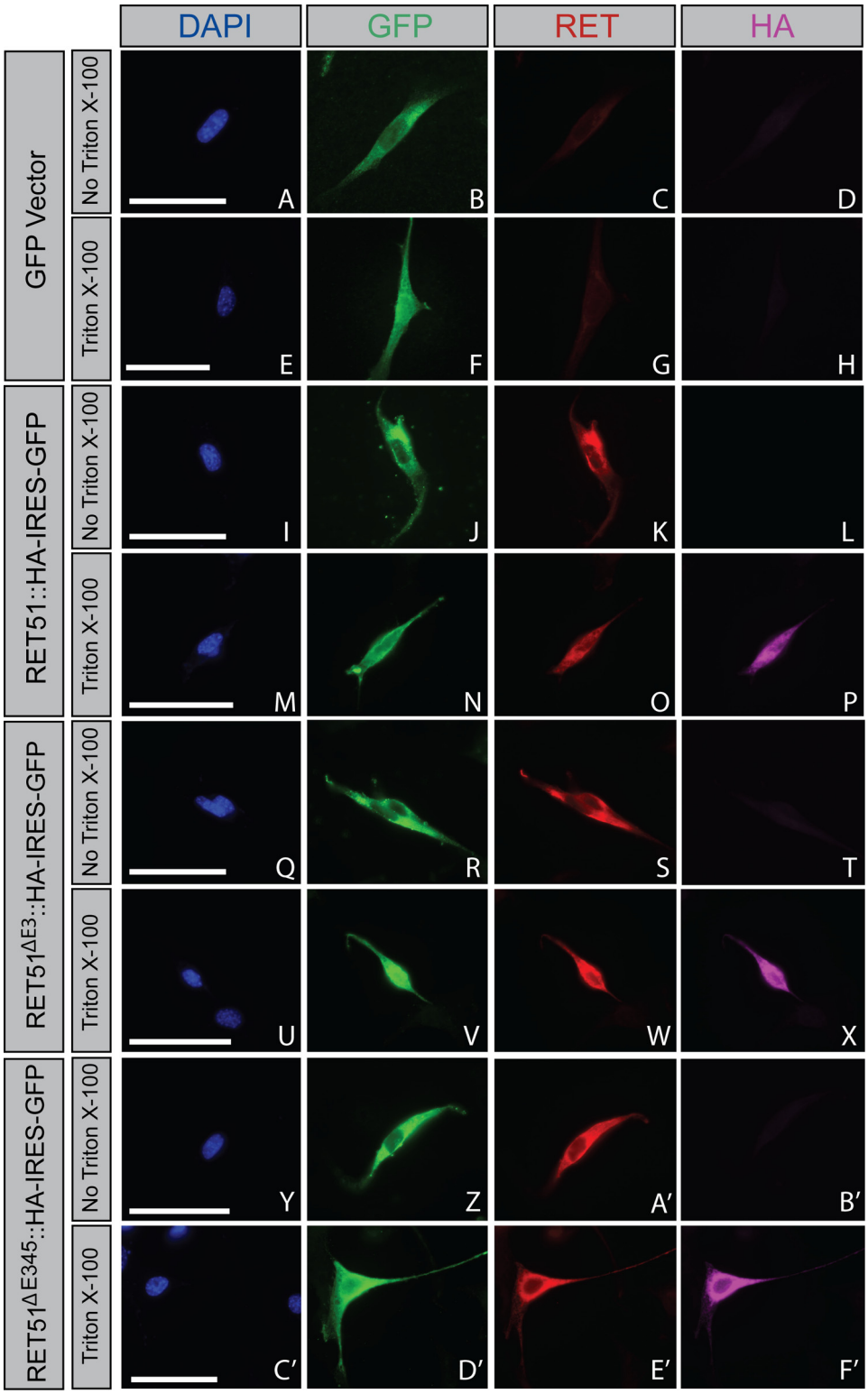


FIGURE 3. **RET$^{\Delta E3}$ and RET$^{\Delta E345}$ are trafficked to the cell surface.** NIH/3T3 cells were transfected with *GFP* (*A–H*), *Ret51::HA* (*I–P*), *Ret51*$^{\Delta E3}$*::HA* (*Q–X*), or *Ret51*$^{\Delta E345}$*::HA* (*Y–F′*). Constructs for the RET51 isoforms were bicistronic, allowing for expression of GFP as an indicator for positive transfection, which was encoded by an IRES-GFP following RET cDNA sequences. Cells were washed in 1× PBS and fixed briefly in 4% paraformaldehyde 24 h post-transfection. Cells were then blocked in immunofluorescence blocking solution with or without Triton X-100 to allow for cell membrane permeabilization. In the absence of Triton X-100, antibodies specific for the RET extracellular domain were able to bind to RET51::HA (*K*), RET51$^{\Delta E3}$::HA (*S*), and RET51$^{\Delta E345}$::HA (*A′*). However, using an antibody against the HA epitope that would detect the C terminus located intracellularly for RET51::HA (*L*), RET51$^{\Delta E3}$::HA (*T*), and RET51$^{\Delta E345}$::HA (*B′*) showed no binding/fluorescence in the absence of Triton X-100. When immunofluorescence blocking solution with Triton X-100 was used, fluorescence was detected using the anti-HA antibody for RET51::HA (*P*), RET51$^{\Delta E3}$::HA (*X*), and RET51$^{\Delta E345}$::HA (*F′*). These data show that RET51$^{\Delta E3}$ and RET51$^{\Delta E345}$ are trafficked to the cell surface similarly as full-length RET51. *Scale bars* represent 20 $\mu$m.

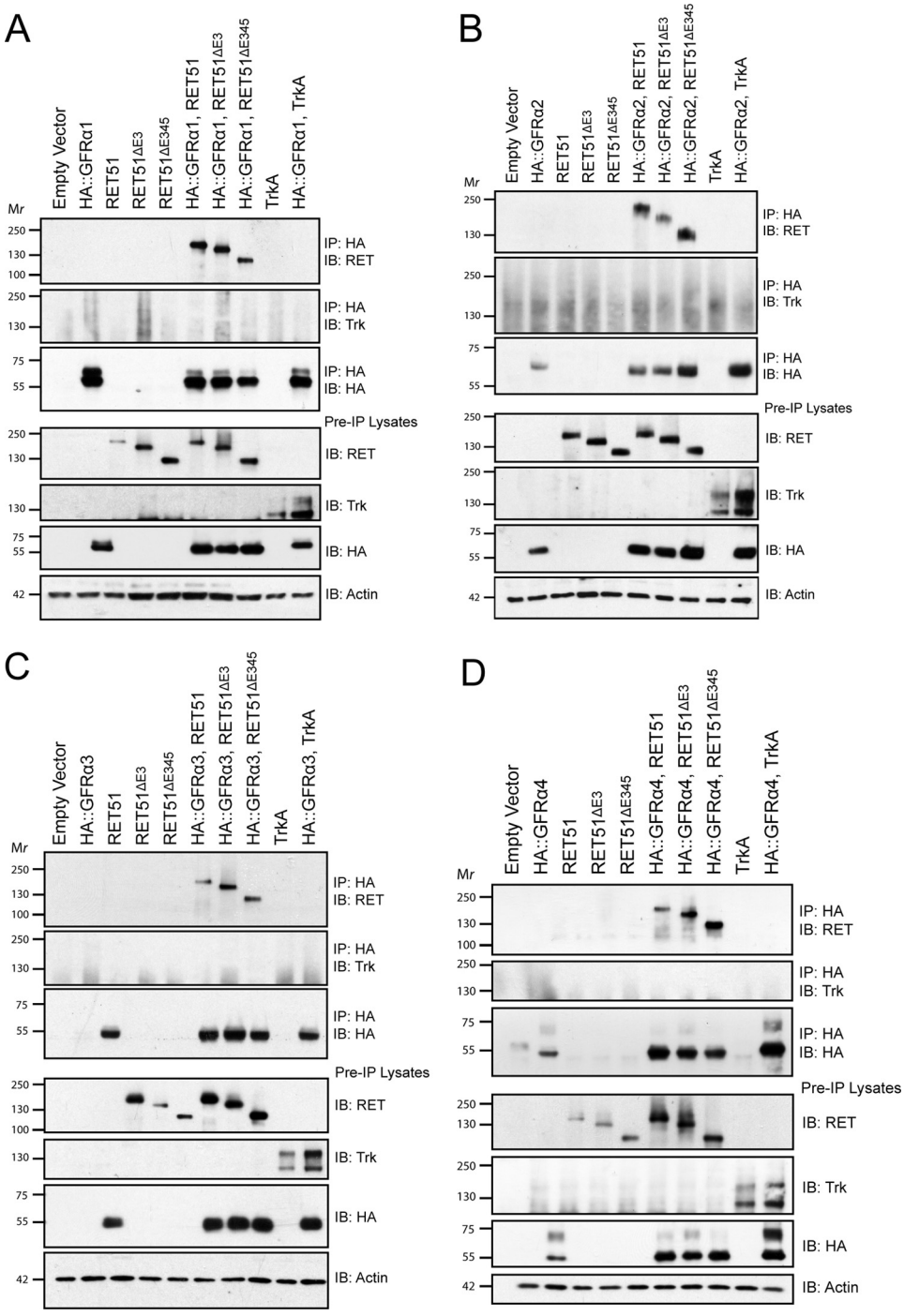


FIGURE 4. **RET$^{\Delta E3}$ and RET$^{\Delta E345}$ bind to GFRα1, GFRα2, GFRα3, and GFRα4.** *RET51*, *RET51*$^{\Delta E3}$, and *RET51*$^{\Delta E345}$ were co-transfected with HA epitope-tagged *GFRα1* (*A*), *GFRα2* (*B*), *GFRα3* (*C*), or *GFRα4* (*D*). Immunoprecipitations (*IP*) were performed using an HA antibody to select for GFRαs. Immunoblotting (*IB*) for RET showed interaction of RET51$^{\Delta E3}$ and RET51$^{\Delta E345}$ with all four GFRα proteins. Co-transfection of HA::GFRα1, HA::GFRα2, HA::GFRα3, or HA::GFRα4 with TrkA was performed as a negative control, and, as expected, TrkA did not associate with any of the GFRαs.

(Tyr(P)) between the RET isoforms and individually evaluated phosphorylation at two tyrosine residues of RET, Tyr$^{905}$ and Tyr$^{1062}$. Tyrosine 905 in the RET kinase domain is an autocatalytic tyrosine that is conserved in many receptor tyrosine kinases and is a binding site for GRB7 and GRB10 (36–38). Additionally, mutation of tyrosine 905 to phenylalanine (Y905F) impairs the kinase activity of RET (39). Tyrosine 1062 is a binding site for SHC, Dok4/5, IRS-1, and FRS-2 when phosphorylated and is a binding site for Enigma in a phosphorylation-independent manner (36, 40–47). Interaction between Tyr$^{1062}$ and these adaptor proteins leads to activation of the Ras/ERK and PI3K/AKT pathways (41, 42, 45, 46, 48).

To evaluate RET phosphorylation, NIH/3T3 cells were transfected with *RET51*, *RET51*$^{\Delta E3}$, or *RET51*$^{\Delta E345}$ constructs in the presence or absence of *GFRα1*, and the total levels of phosphorylated RET or the level of phosphorylation at Tyr$^{905}$ and Tyr$^{1062}$ were assessed. To analyze total Tyr(P) levels of RET, immunoprecipitations of RET51 were performed, followed by immuno-

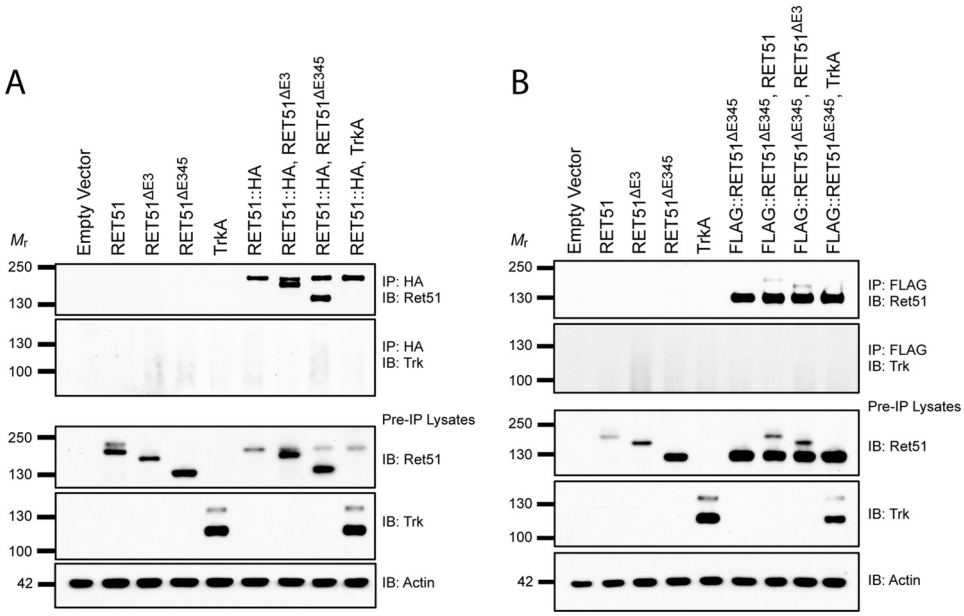


FIGURE 5. **RET$^{\Delta E3}$ and RET$^{\Delta E345}$ can heterodimerize with full-length RET.** *A*, HA epitope tagged *RET51* (*RET51::HA*) was co-transfected with untagged *RET51*$^{\Delta E3}$ or *RET51*$^{\Delta E345}$ in HEK293T cells. Immunoprecipitations (*IP*) were performed with an HA antibody to select for RET51::HA. Immunoblotting (*IB*) for RET51 showed co-immunoprecipitation of RET51$^{\Delta E3}$ and RET51$^{\Delta E345}$ with full-length RET51. *B*, a similar experiment was performed using FLAG epitope tagged *RET51*$^{\Delta E345}$ (*FLAG:: RET51*$^{\Delta E345}$). Immunoprecipitations with an anti-FLAG antibody selected for FLAG:: RET51$^{\Delta E345}$. Immunoblotting for RET51 demonstrated the association of RET51 and RET51$^{\Delta E3}$ with FLAG:: RET51$^{\Delta E345}$. Co-transfections with TrkA were performed for both experiments as a negative control, and immunoblotting for TrkA showed no binding with either RET51::HA or FLAG::RET51$^{\Delta E345}$, as expected.

blotting for Tyr(P) (Fig. 6*A*). An increase in the level of RET$^{\Delta E345}$ phosphorylation compared with full-length RET was observed, but this was not statistically significant ($p = 0.0837$). We did detect, however, a significant increase in the Tyr(P) level of RET$^{\Delta E345}$ co-expressed with GFR$\alpha$1 compared with full-length RET co-expressed with GFR$\alpha$1 ($p = 0.0366$). The phosphorylation of RET$^{\Delta E3}$ co-expressed with GFR$\alpha$1 or expressed alone was not significantly different from full-length Ret ($p = 0.6231$).

To determine levels of Tyr(P)$^{905}$ and Tyr(P)$^{1062}$, pre-immunoprecipitation lysates were collected from samples in the previous experiments, and immunoblotting was performed using antibodies specific for these two phosphorylated tyrosine residues (Fig. 6*B*). Levels of Tyr(P)$^{905}$ and Tyr(P)$^{1062}$ were significantly elevated for RET$^{\Delta E345}$ compared with RET ($p = 0.0439$ and $p = 0.0411$, respectively) and also for RET$^{\Delta E345}$ co-expressed with GFR$\alpha$1 compared with full-length RET co-expressed with GFR$\alpha$1 ($p = 0.0106$ and $p = 0.0096$, respectively). However, levels of Tyr(P)$^{905}$ and Tyr(P)$^{1062}$ were unchanged for RET$^{\Delta E3}$ compared with RET and also for RET$^{\Delta E3}$ co-expressed with GFR$\alpha$1 compared with full-length RET co-expressed with GFR$\alpha$1. Taken together, these data suggest that RET$^{\Delta E3}$ has a similar activation level as full-length RET, whereas RET$^{\Delta E345}$ has an elevated activation level compared with RET in a ligand-independent manner. Additionally, the lower total phosphotyrosine level for RET$^{\Delta E345}$ compared with Tyr(P)$^{905}$ and Tyr(P)$^{1062}$ suggests that one or more of the other tyrosine residues in RET is not phosphorylated as highly as Tyr$^{905}$ and Tyr$^{1062}$ compared with full-length RET.

Because we consistently observed an increased level of tyrosine phosphorylation of the RET$^{\Delta E345}$ isoform compared with full-length RET, we wondered whether this level of receptor activation was similar to oncogenic RET mutations, particularly those found in MEN2. Human *RET* point mutations known to be causal for either MEN2A or MEN2B were introduced into the *RET51* expression plasmid, specifically C634R (RET51$^{MEN2A}$) and M918T (RET51$^{MEN2B}$). NIH/3T3 cells were transfected with *RET51*, *RET51*$^{\Delta E3}$, *RET51*$^{\Delta E345}$, *RET51*$^{MEN2A}$, or *RET51*$^{MEN2B}$ constructs. Immunoprecipitations for RET51 were performed to isolate RET proteins, followed by immunoblotting for Tyr(P) as described previously. We observed a significant increase in the level of phosphorylation of both RET$^{MEN2A}$ and RET$^{MEN2B}$ oncogenic proteins compared with full-length RET ($p = 0.0282$ and $p = 0.0097$, respectively) (Fig. 6*F*). The levels of phosphorylation of RET$^{MEN2A}$ and RET$^{MEN2B}$ compared with RET$^{\Delta E345}$ showed no significant difference ($p = 0.4898$ and $p = 0.1712$, respectively). These data indicate that the RET$^{\Delta E345}$ isoform is phosphorylated at similar levels as oncogenic RET mutations.

*RET*$^{\Delta E3}$ *Is Activated in a GDNF-dependent Manner but RET*$^{\Delta E345}$ *Is Not*—Although differences are observed in the level of ligand-independent activation for RET$^{\Delta E3}$ and RET$^{\Delta E345}$, we wondered whether these two receptors could be activated in a GDNF-dependent manner. To evaluate this, Neuro2A cells were co-transfected with HA epitope-tagged *RET51*, *RET51*$^{\Delta E3}$, or *RET51*$^{\Delta E345}$ and with untagged *GFR$\alpha$1*. Twenty-four hours post-transfection, the culture medium was removed, and cells were stimulated with 200 ng/ml recombinant mouse GDNF for 30 min. Cells were detergent-extracted, and immunoprecipitations for HA were performed to isolate the exogenous RET isoforms. Immunoblotting for GFR$\alpha$1 was performed to determine the level of GDNF-dependent association of GFR$\alpha$1 to RET (Fig. 7*A*). For our positive control, where GFR$\alpha$1 and RET51 were co-expressed, we observed a significant GDNF-dependent association of these proteins after 30 min of stimulation ($p = 0.0373$) (Fig. 7*B*). Under conditions

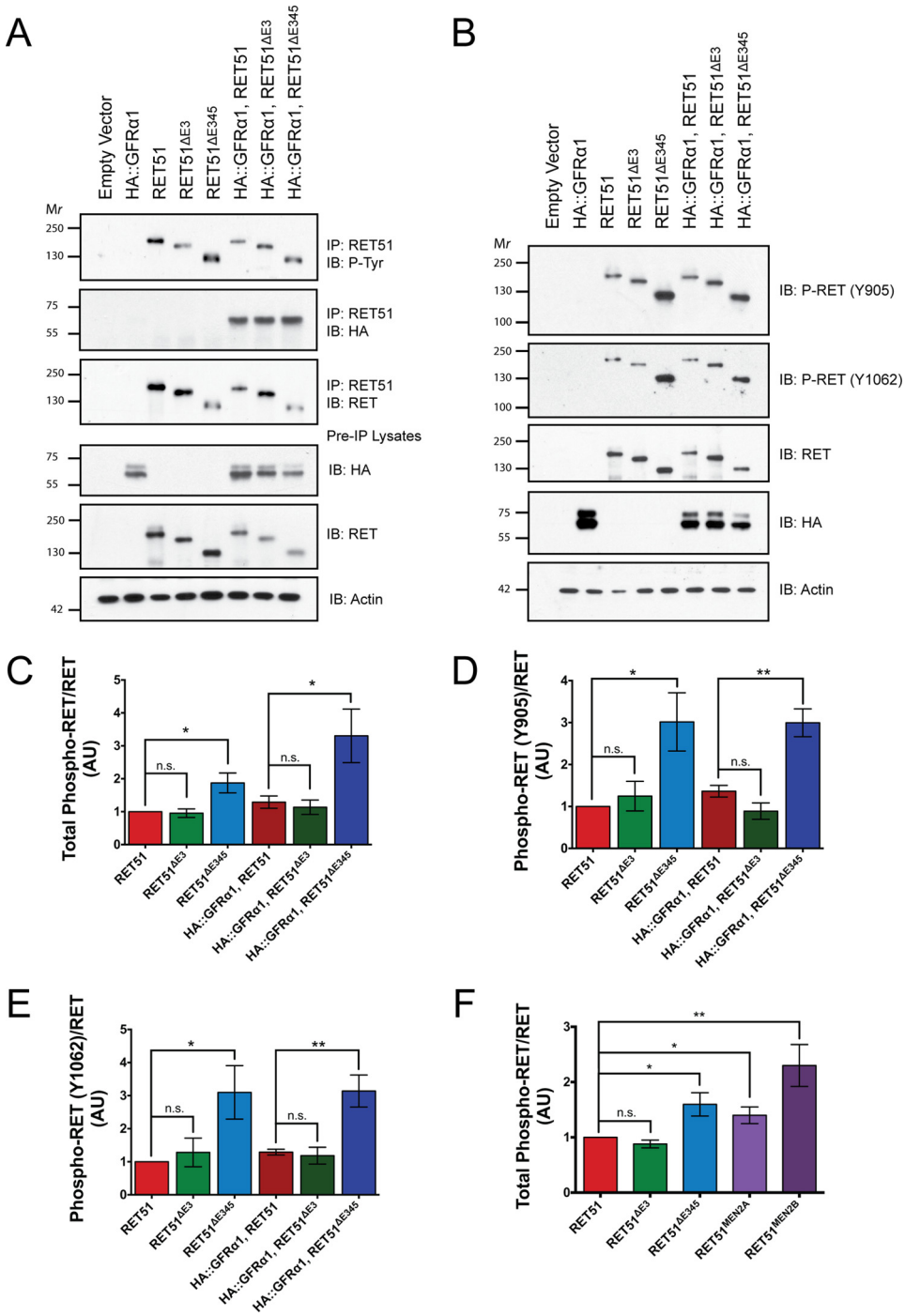


FIGURE 6. **RET$^{\Delta E345}$ displays increased ligand-independent activation compared with full-length RET.** *A*, *RET51* was co-transfected with HA epitope-tagged *GFRα1* in NIH/3T3 cells. Immunoprecipitations (*IP*) were performed with a RET51 antibody to select for the RET isoforms. Immunoblotting (*IB*) for phospho-tyrosine and RET was performed, and integrated density values were calculated for each. *B*, preimmunoprecipitation lysates from the previous experiment were subjected to SDS-PAGE, and Western blotting was performed to determine the levels of residue-specific tyrosine phosphorylation of RET. Immunoblotting was performed for phospho-RET (Tyr$^{905}$), phospho-RET (Tyr$^{1062}$), and RET, and integrated density values were calculated for each. Ratios of phospho-RET/RET (*C*), phospho-RET (Tyr$^{905}$)/RET (*D*), and phospho-RET (Tyr$^{1062}$)/RET (*E*) are reported, with values normalized to RET51. *F*, expression plasmids encoding oncogenic RET proteins, RET51$^{MEN2A}$ and RET51$^{MEN2B}$, were transfected into NIH/3T3 cells, and integrated density values were calculated and analyzed for phospho-RET/RET for all RET isoforms. *, $p < 0.05$; **, $p < 0.01$; *n.s.*, not significant.

where GFRα1 and RET51$^{\Delta E3}$ or RET51$^{\Delta E345}$ were co-expressed, we observed a trend of GDNF-dependent association of GFRα1 to both RET isoforms, but this ligand-dependent interaction was not statistically significant ($p = 0.1750$ and $p = 0.3269$, respectively).

To determine whether the RET isoforms were activated in a GDNF-dependent manner, immunoblotting for poly-ubiquitin was performed. We have shown previously that, upon ligand activation and autophosphorylation, RET is rapidly poly-ubiquitinated and targeted for degradation (49). Because ectopic

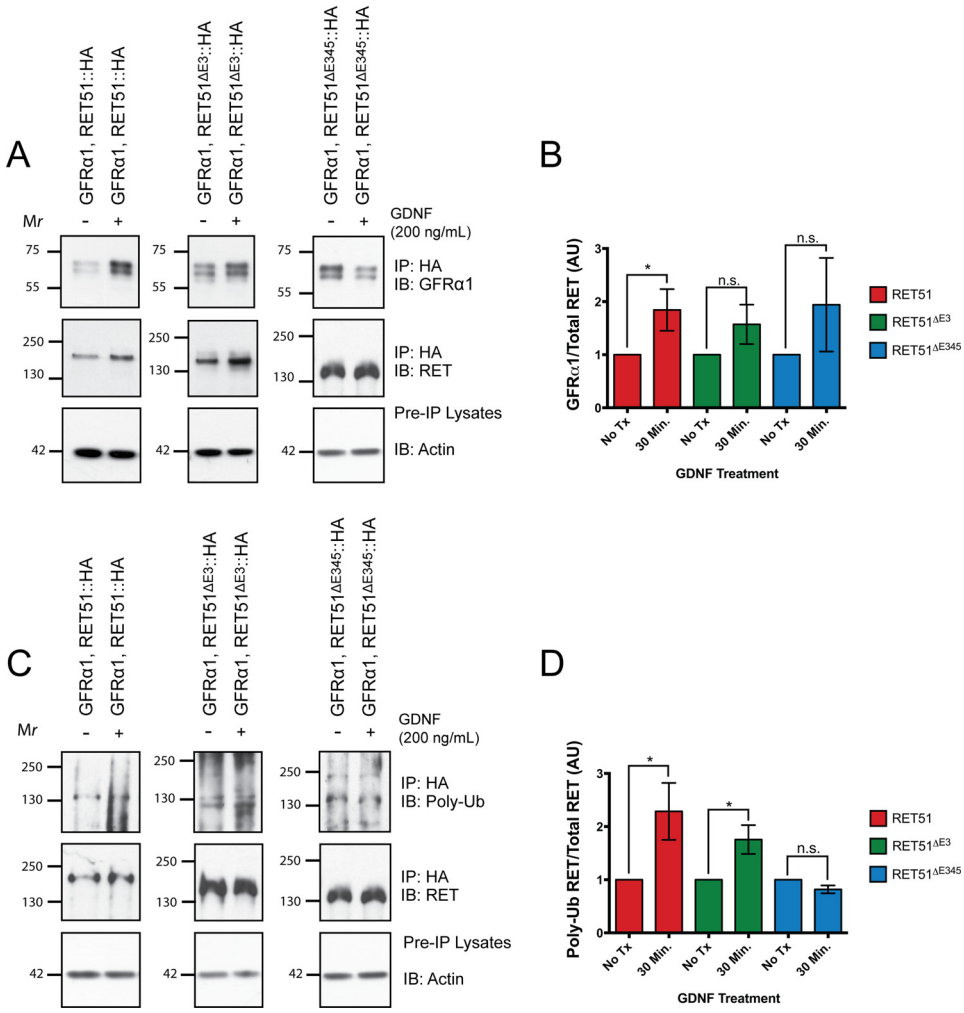


FIGURE 7. **RET$^{\Delta E3}$ is activated in a GDNF-dependent manner but RET$^{\Delta E345}$ is not.** *A*, HA epitope-tagged *RET* constructs were co-transfected with *GFRα1* into Neuro2A cells. Twenty-four hours post-transfection, the medium was removed, and fresh medium was added to cells containing 200 ng/ml GDNF. Cells were stimulated for 30 min, and immunoprecipitations (*IP*) were performed from lysates with an HA antibody to selectively pull down the RET isoforms. Immunoblotting (*IB*) for GFRα1 and RET was performed, and integrated density values were calculated for each. *B*, quantification the of GFRα1/RET ratios. *C*, immunoblotting for poly-ubiquitin was performed, and integrated density values were calculated for poly-ubiquitinated RET and total RET. *D*, quantification of poly-ubiquitinated RET/RET ratios. *n.s.*, not significant. *AU* is arbitrary units. *No Tx* indicates cells that were not stimulated with GDNF. *Asterisks* indicate $p < 0.05$.

expression of RET results in high levels of autophosphorylation in the absence of ligand, we were not able to use phosphotyrosine immunoblotting as a measure of RET activation upon GDNF stimulation. We observed a significant increase in poly-ubiquitinated RET51 ($p = 0.0370$) following GDNF stimulation, as expected, and also observed a significant increase in poly-ubiquitinated RET51$^{\Delta E3}$ ($p = 0.0493$), suggesting that this isoform is activated in a GDNF-dependent manner. Interestingly, we did not observe a difference in the level of poly-ubiquitinated RET51$^{\Delta E345}$ following GDNF stimulation ($p = 0.0696$). These data suggest that, like full-length RET, RET$^{\Delta E3}$ is activated in a GDNF-dependent manner but RET$^{\Delta E345}$ is not.

## Discussion

Alternative splicing of precursor mRNA is one of many processes that mediates gene regulation in metazoans, and the frequency of alternative splicing increases with species complexity (50, 51). For example, of the ~25,000 genes encoded by the human genome, ~95% produce transcripts that are alternatively spliced (50, 51). By expanding the proteome through the synthesis of various protein isoforms, alternative splicing allows for increased protein diversity, with isoforms performing different biological functions.

Here we provide evidence for two alternative splicing events in *Ret* that, in combination with *Ret9* or *Ret51* alternative splicing, give rise to at least five *Ret* transcripts (Fig. 2*C*). The splicing events for *RET$^{\Delta E3}$* and *RET$^{\Delta E345}$* have only been described previously in human tissues (12). Because an additional *Ret* transcript, *RET43*, is only expressed in humans, we examined the expression of *RET$^{\Delta E3}$* and *RET$^{\Delta E345}$* in additional vertebrate tissues to determine whether these might also be human-specific transcripts (8, 52). To this end, we discovered that *RET$^{\Delta E3}$* and *RET$^{\Delta E345}$* are not human-specific *RET* transcripts but are also expressed in normal developing tissues of zebrafish, mice, and rats (Fig. 1*C*). Functionally important transcripts are transcriptionally conserved between species, arguing that *RET$^{\Delta E3}$* and *RET$^{\Delta E345}$* have physiologically important functions.

Analysis of an experimentally validated structural model for the RET cadherin-like domains 1–4 was made to evaluate the

consequence of exon deletions of *RET* alternative splicing on the ligand binding and activation characteristics of RET$^{\Delta E3}$ and RET$^{\Delta E345}$ (Fig. 1*B*). Previous experiments indicate that the GDNF-GFR$\alpha$1 complex binds directly to CLD4 and the cysteine-rich domain (53). This suggested that both RET$^{\Delta E3}$ and RET$^{\Delta E345}$ should be able to bind to the GDNF-GFR$\alpha$1 complex, and indeed this interaction was observed not only for GFR$\alpha$1 but also for GFR$\alpha$2, GFR$\alpha$3, and GFR$\alpha$4 (Fig. 4). It should be noted that, in our experiments, the chicken *GFR$\alpha$4* construct contained all three cysteine-rich domains, unlike mammalian GFR$\alpha$4, which lacks domain 1. Although it was originally thought that CLD1–3 of RET was involved in direct binding from results obtained through mutagenesis studies, a direct interaction between CLD1–3 and the GDNF-GFR$\alpha$1 complex has not been observed (53, 54). Instead, it has been proposed that CLD1–3 contributes to the stability of the tertiary structure of the GDNF-GFR$\alpha$1-RET complex by forming a secondary dimerization site to trap the GDNF-GFR$\alpha$1 binary complex (14). These studies predict that RET$^{\Delta E3}$, which forms a fused CLD1-CLD2 region, likely gives rise to a less stable tertiary GDNF-GFR$\alpha$1-RET complex compared with full-length RET. This may result in a receptor variant with differential ligand binding specificities. FGF receptors are a subfamily of four receptor tyrosine kinases that are receptors for FGFs, of which there are 18 ligands (55). Alternative splicing of the FGF receptors in the region coding for the extracellular ligand-binding domain of the receptors allows for differential ligand binding. It is possible that the alternative splicing responsible for *RET$^{\Delta E3}$* similarly modifies GFL-GFR$\alpha$ affinity. Alternatively, the truncated extracellular domain of RET$^{\Delta E3}$ may cause alterations in the conformational changes that occur upon GFL-GFR$\alpha$ binding that induces receptor autophosphorylation. This would cause different autophosphorylation kinetics in *RET$^{\Delta E3}$* compared with full-length *RET* and, therefore, differential activation of downstream second messenger cascades. Biochemical experiments using an *in vitro* system that allows for the monitoring of autophosphorylation upon direct ligand activation of *RET$^{\Delta E3}$* or full-length *RET* in isolation will be necessary to distinguish between these possibilities.

The large deletion in the extracellular domain of RET$^{\Delta E345}$, including the $Ca^{2+}$ binding domain, which is important for RET folding and ligand-dependent signaling, is predicted to have dramatic effects on RET$^{\Delta E345}$ activation. Indeed, it is likely that RET$^{\Delta E345}$ functions as a constitutively active form of RET, consistent with the mechanistic data shown in Fig. 6. Autophosphorylation of RET$^{\Delta E345}$ is increased compared with full-length RET in the presence and absence of GFR$\alpha$1 *in vitro* (Fig. 6*B*). Constitutively active receptor tyrosine kinases have not been found in normal tissues and usually arise from germline and somatic mutations, where they are most commonly found to cause neoplasia. Activating mutations in RET have been shown to be responsible for multiple endocrine neoplasia, type 2, including neoplasias such as medullary thyroid carcinoma and pheochromocytomas (56). Unlike other constitutively active forms of RET, RET$^{\Delta E345}$ may be posttranscriptionally or translationally regulated *in vivo* in a manner that is not recapitulated in the *in vitro* system used here. In this way, the signaling of RET$^{\Delta E345}$ may be under tight regulation for this isoform to perform specific functions *in vivo*.

To interrogate the functions of RET$^{\Delta E3}$ and RET$^{\Delta E345}$ in primary neurons and tissues, we attempted to generate isoform-specific antibodies. Likewise, we also tried to create siRNAs to selectively knock down *Ret$^{\Delta E3}$* and *Ret$^{\Delta E345}$* transcripts. Neither of these experimental approaches were successful at targeting RET$^{\Delta E3}$ and RET$^{\Delta E345}$ without also affecting full-length RET. Therefore, to determine the physiologic functions of RET$^{\Delta E3}$ and RET$^{\Delta E345}$, a transgenic approach in a vertebrate will be required to selectively remove these individual transcripts. This could be accomplished by deleting specific introns and fusing the flanking exons in-frame to inhibit exon skipping (*e.g.* remove intron 3 and fuse exons 2 and 3 together to inhibit alternative splicing for *Ret$^{\Delta E3}$*). How this approach would affect RET expression and other splicing events, however, is unknown. In addition, because of the invariably coincident expression of *Ret$^{\Delta E3}$* and *Ret$^{\Delta E345}$* in the same tissues as *Ret*, it is possible that full-length RET may compensate for the functions of RET$^{\Delta E3}$ and RET$^{\Delta E345}$. As an alternative approach, production of knockin animals in which only *Ret$^{\Delta E3}$* or *Ret$^{\Delta E3}$* is expressed would determine whether these isoforms are capable of supporting the normal development of the nervous system and kidneys.

Last, to gain a mechanistic understanding of the factors responsible for the alternative splicing of *Ret,* it would be interesting to explore RNA motifs encoding exon splicing enhancers within the locus that impact the formation of *Ret$^{\Delta E3}$* and *Ret$^{\Delta E345}$*. Understanding the spliceosome machinery involved in this process may help us understand why the expression of these transcripts are elevated in tumors, such as in pheochromocytomas (12). Overall, it may be necessary to return to a disease model, such as neuroendocrine gland tumors, where these *RET* transcripts were originally identified and use the pathobiology to understand the signaling capacities of RET$^{\Delta E3}$ and RET$^{\Delta E345}$ to identify their functions in normal development.

## Experimental Procedures

*Molecular Modeling*—This analysis was performed as described previously (14). Models of cadherin-like domains 1–4 were taken from PDB code 4UX8, defined by a combination of EM and small angle x-ray scattering analyses. The figure was made using PyMOL software (Schrödinger).

*RNA Isolation, RT-PCR, and qPCR*—Total RNA was isolated from zebrafish, mouse, or rat tissues using TRIzol reagent (Thermo Fisher Scientific) according to the instructions of the manufacturer. cDNA synthesis was performed from 1 $\mu$g of total RNA to generate poly(A) first-strand cDNA using the SuperScript III First-Strand Synthesis System for RT-PCR kit (Life Technologies). For RT-PCR reactions with amplicons of less than 200 bp, GoTaq Green Master Mix (Promega) and species-specific oligonucleotide primers for *Ret*, *Ret$^{\Delta 3}$*, and *Ret$^{\Delta 345}$* were used. RT-PCR reactions with amplicons greater than 200 bp were performed using the Phusion high-fidelity DNA polymerase kit (New England Biolabs) following the instructions of the manufacturer. qPCR was performed using FastStart Universal SYBR Green Master Mix (Roche) and run on a Quant-

Studio 6 Flex real-time PCR system (Thermo Fisher Scientific). Quantitative analyses were performed by calculating the ΔCt (Ct of transcript divided by Ct of the housekeeping gene *actin*) for each gene analyzed and transforming that value to $\log_2$. These values are reported as the relative expression.

*Primer Sequences*—The primers used for this study were as follows: ZF.RetFL.F, 5′-TCG TAG TTT ACG CAG CGG CTC A-3′; ZF.RetFL.R, 5′-TCG CGA TTT TCA GTG ATG TG-3′; ZF.Ret3.F, 5′-CAG TAG TTT ACG ATC TTC TGT ACC G-3′; ZF.Ret3.R, 5′-TTC AGT GTC AGT CCC GTT GA-3′; ZF.Ret345.F, 5′-CAG TAG TTT ACA GCT GAA ACT CAG TC-3′; ZF.Ret345.R, 5′-TGA CAT TGG AGA AGC GAA TG-3′; Mouse.RetFL.F, 5′-AGC ATC CGC AAT GGT GGT TT-3′; Mouse.RetFL.R, 5′-TGT TCT CCC TGA CTC GGA AG-3′; Mouse.Ret3.F, 5′-AGC ATC CGC AGG GAT AGT CT-3′; Mouse.Ret3.R, 5′-ACA CTG TCA CTG GGA AGG AC-3′; Mouse.Ret345.F, 5′-AGC ATC CGC AAG CTG ATT CT-3′; Mouse.Ret345.R, 5′-TTC ACT GGG AAG GAG TAG GC-3′; Rat.RetFL.F, 5′-AGC ATC CGC AAT GGC GGC TT-3′; Rat.RetFL.R, 5′-TAG CAT GCG GAA CTG GTA GA-3′; Rat.Ret3.F, 5′-AGC ATC CGC AGG GAC GGT CT-3′; Rat.Ret3.R, 5′-CCG CTT AAA CTC CAC CAC AG-3′; Rat.Ret345.F, 5′-AGC ATC CGC AAG CTG GTT CT-3′; Rat.Ret345.R, 5′-TAG GCC ATG GGT AGG TTC AG-3′; Mouse.Ret9.R, 5′-ATT TAC TGT CCA TTG CAA GGC-3′; and Mouse.Ret51.R, 5′-CCT ATC AGT GCT TTA AGT CTG-3′.

*Mice*—Wild-type C57BL/6J mice were purchased from The Jackson Laboratories (Bar Harbor, ME). $Ret^{-/-}$ mice have been described previously and were maintained in a mixed genetic background (57). For timed matings, noon of the day on which a vaginal plug was detected was considered E0.5. All housing and procedures performed on mice were approved by the University of Michigan Animal Care and Use Committee.

*Detergent Extraction and Preclearing of Whole Tissues*—Tissues were harvested, placed in a 2-ml tube with 250 μl of immunoprecipitation buffer lacking Nonidet P-40 (TBS (pH 7.4), 10% glycerol, 500 μM sodium vanadate, and protease inhibitors) along with a steel grinding ball (5 mm, 69989, Qiagen, Valencia, CA) and mechanically homogenized using a TissueLyzer II (Qiagen) for 2 min at a frequency of 20 Hz. Following this, 250 μl of 2% Nonidet P-40-containing immunoprecipitation buffer was added to homogenates and incubated for 1 h at 4 °C under gentle agitation. Homogenates were then centrifuged for 10 min at 16,000 × *g* and subjected to an initial preclearing step with protein A and protein G alone at 4 °C for 2 h under gentle agitation. A second preclearing step was performed with protein A, protein G, and a species-matched nonspecific control IgG for 2 h under gentle agitation.

*Immunoprecipitations and Immunoblotting*—Plates were placed on ice, gently washed twice with 1× PBS (pH 7.4), and lysed with modified radioimmune precipitation assay buffer (TBS (pH 7.4), 10% glycerol, 1% Triton X-100, 0.1% SDS, 500 μM sodium vanadate, and protease inhibitors). Proteins were immunoprecipitated using anti-RET9 (goat, Santa Cruz Biotechnology), anti-RET51 (goat, Santa Cruz Biotechnology), anti-HA (mouse, Millipore), or anti-FLAG (rabbit, Cell Signaling Technology) selective antibodies. Immunoprecipitates were subjected to SDS-PAGE, followed by electroblotting onto PVDF membranes (Immobilon P, Millipore). Immunoblotting was performed on blots using antibodies selective for RET (1:500, goat, R&D Systems), HA (1:5000, rabbit, Cell Signaling Technology), Trk (1:1000, rabbit, Santa Cruz Biotechnology), phospho-tyrosine (1:1000, mouse, Millipore), phospho-RET ($Tyr^{905}$) (1:500, rabbit), phospho-RET ($Tyr^{1062}$, 1:500, rabbit), GFRα1 (1:500, goat, R&D Systems), or poly-ubiquitin (1:500, mouse, Enzo Life Sciences). Phospho-RET ($Tyr^{905}$) and phospho-RET ($Tyr^{1062}$) have been described previously (58). Lysates collected prior to immunoprecipitations served as loading controls to assess protein expression levels and were also subjected to immunoblotting for actin (1:1000, goat, Santa Cruz Biotechnology). Each biochemical experiment was performed three to four times with similar results.

*Mammalian Cell Culture and Transfections*—NIH/3T3 (ATCC), HEK293T (ATCC), and Neuro2A cells (ATCC) were maintained at 37 °C with 5% $CO_2$ in DMEM supplemented with FBS (10% by volume) and a penicillin/streptomycin/glutamine mixture. Cells were plated into 6-well tissue culture plates and allowed to proliferate until cells were 70% confluent. Transfections of cells were performed using Lipofectamine 2000 according to the instructions of the manufacturer (Invitrogen). For experiments testing the interaction of proteins, a total of 4 μg of plasmid DNA was added per well using a GFP plasmid as a control for transfecting equal amounts of DNA. For *in vitro* ligand-independent activation experiments, 2 μg of *HA::GFRα1* and 1 μg of one of the *RET* constructs were transfected for a total of 3 μg of DNA per condition, with a *GFP* plasmid used as a control for transfecting equal amounts of DNA. $RET51^{\Delta E3}$ and $RET51^{\Delta E345}$ constructs were subcloned from *RET51* constructs into pcDNA3.1 (Thermo Fisher Scientific). A *Ret51* construct encoding mouse RET51 fused at the C terminus with an HA epitope tag (RET51::HA) was acquired from Dr. Ben Allen. This plasmid was subcloned to create similarly tagged $Ret51^{\Delta E3}$ and $Ret51^{\Delta E345}$ constructs, which were subcloned into pLentilox-IRES-GFP (University of Michigan Vector Core). For *in vitro* ligand-dependent activation experiments, 3 μg of HA epitope-tagged *Ret51*, $Ret51^{\Delta E3}$, or $Ret51^{\Delta E345}$ was co-transfected with 3 μg of untagged *GFRα1*. Twenty-four hours post-transfection, the medium was aspirated, and cells were treated with 200 ng/ml recombinant mouse GDNF (Peprotech) in fresh cell culture medium for 30 min. The HA::GFRα1 (mouse) plasmid was generously donated by Dr. Ben Allen. The HA::GFRα2 (rat), HA::GFRα3 (mouse), and HA::GFRα4 (chicken) plasmids were generously donated by Dr. Carlos Ibáñez. The TrkA (rat) plasmid was generously donated by Dr. Christin Carter-Su. Constructs encoding human RET51 harboring MEN2A (C634R) and MEN2B (M918T) point mutations in *RET* were created using the QuikChange II XL site-directed mutagenesis kit (Agilent).

*Quantification of Immunoblots*—Scanned images of x-ray films were imported into ImageJ (National Institutes of Health) and processed using the gel analysis tool. Integrated density values obtained from immunoblotting were reported as mean ± S.E. with arbitrary units on the vertical axis. Values were normalized to the level of RET51 phosphorylation in each experiment. Statistical analyses were performed using

Student's *t* test for each experiment, and all biochemical experiments were performed at least three times with similar results.

*Immunocytochemistry*—Transfected cells that were plated on glass coverslips were fixed for 8 min in 4% paraformaldehyde. Cells were washed twice in 1× PBS and briefly blocked in immunofluorescence blocking solution (3% BSA and 1% normal donkey serum in 1× PBS (pH 7.4)) with or without 0.1% Triton X-100. Primary antibodies were diluted in blocking buffer (RET (1:50, goat, R&D Systems), HA (1:1000, mouse, Millipore)), and slides were incubated at 4 °C overnight. Cells were washed twice with 1× PBS and then incubated at room temperature for 1 h with secondary antibodies (donkey anti-mouse Alexa Fluor 633 (Thermo Fisher Scientific), donkey anti-goat 543 (Biotium)) diluted in blocking solution. Last, cells were washed three times in 1× PBS and mounted with DAPI Fluoromount-G (Southern Biotech). Cells were imaged using a Zeiss Axiovert 200 M epifluorescence microscope with a ×40 objective.

*Author Contributions*—N. A. G. conducted the experiments, analyzed the results, and wrote the paper. J. K. V. and S. S. N. performed experiments. N. Q. M. performed the structure-based predictions of the impact of exon deletions. B. A. P. conceived the idea for the project, contributed intellectual advice, and edited the manuscript.

*Acknowledgments—We thank Dr. Benjamin Allen for reagents and critical scientific comments on the manuscript. Additionally, we thank Dr. Carlos Ibáñez, Dr. Christin Carter-Su, and Dr. Frank Costantini for reagents. We also thank the Pierchala laboratory for helpful scientific discussions.*

## References

1. Airaksinen, M. S., and Saarma, M. (2002) The GDNF family: signalling, biological functions and therapeutic value. *Nat. Rev. Neurosci.* **3,** 383–394
2. Baloh, R. H., Enomoto, H., Johnson, E. M., Jr., and Milbrandt, J. (2000) The GDNF family ligands and receptors-implications for neural development. *Curr. Opin. Neurobiol.* **10,** 103–110
3. Meng, X., Lindahl, M., Hyvönen, M. E., Parvinen, M., de Rooij, D. G., Hess, M. W., Raatikainen-Ahokas, A., Sainio, K., Rauvala, H., Lakso, M., Pichel, J. G., Westphal, H., Saarma, M., and Sariola, H. (2000) Regulation of cell fate decision of undifferentiated spermatogonia by GDNF. *Science* **287,** 1489–1493
4. Naughton, C. K., Jain, S., Strickland, A. M., Gupta, A., and Milbrandt, J. (2006) Glial cell-line derived neurotrophic factor-mediated RET signaling regulates spermatogonial stem cell fate. *Biol. Reprod.* **74,** 314–321
5. Airaksinen, M. S., Titievsky, A., and Saarma, M. (1999) GDNF family neurotrophic factor signaling: four masters, one servant? *Mol. Cell. Neurosci.* **13,** 313–325
6. Wells, S. A., Jr., Santoro M. (2009) Targeting the RET pathway in thyroid cancer. *Clin. Cancer Res.* **15,** 7119–7123
7. de Graaff, E., Srinivas, S., Kilkenny, C., D'Agati, V., Mankoo, B. S., Costantini, F., and Pachnis, V. (2001) Differential activities of the RET tyrosine kinase receptor isoforms during mammalian embryogenesis. *Genes Dev.* **15,** 2433–2444
8. Carter, M. T., Yome, J. L., Marcil, M. N., Martin, C. A., Vanhorne, J. B., and Mulligan, L. M. (2001) Conservation of RET proto-oncogene splicing variants and implications for RET isoform function. *Cytogenet. Cell Genet.* **95,** 169–176
9. Tahira, T., Ishizaka, Y., Itoh, F., Sugimura, T., and Nagao, M. (1990) Characterization of ret proto-oncogene mRNAs encoding two isoforms of the protein product in a human neuroblastoma cell line. *Oncogene* **5,** 97–102
10. Tsui-Pierchala, B. A., Milbrandt, J., and Johnson, E. M., Jr. (2002) NGF utilizes c-Ret via a novel GFL-independent, inter-RTK signaling mechanism to maintain the trophic status of mature sympathetic neurons. *Neuron* **33,** 261–273
11. Tsui, C. C., and Pierchala, B. A. (2010) The differential axonal degradation of Ret accounts for cell-type-specific function of glial cell line-derived neurotrophic factor as a retrograde survival factor. *J. Neurosci.* **30,** 5149–5158
12. Lorenzo, M. J., Eng, C., Mulligan, L. M., Stonehouse, T. J., Healey, C. S., Ponder, B. A., and Smith, D. P. (1995) Multiple mRNA isoforms of the human RET proto-oncogene generated by alternative splicing. *Oncogene* **10,** 1377–1383
13. Anders, J., Kjar, S., and Ibáñez, C. F. (2001) Molecular modeling of the extracellular domain of the RET receptor tyrosine kinase reveals multiple cadherin-like domains and a calcium-binding site. *J. Biol. Chem.* **276,** 35808–35817
14. Goodman, K. M., Kjær, S., Beuron, F., Knowles, P. P., Nawrotek, A., Burns, E. M., Purkiss, A. G., George, R., Santoro, M., Morris, E. P., and McDonald, N. Q. (2014) RET recognition of GDNF-GFRα1 ligand by a composite binding site promotes membrane-proximal self-association. *Cell Rep.* **8,** 1894–1904
15. Kjaer, S., Hanrahan, S., Totty, N., and McDonald, N. Q. (2010) Mammal-restricted elements predispose human RET to folding impairment by HSCR mutations. *Nat. Struct. Mol. Biol.* **17,** 726–731
16. Arenas, E., Trupp, M., Akerud, P., and Ibáñez, C. F. (1995) GDNF prevents degeneration and promotes the phenotype of brain noradrenergic neurons *in vivo*. *Neuron* **15,** 1465–1473
17. Horger, B. A., Nishimura, M. C., Armanini, M. P., Wang, L. C., Poulsen, K. T., Rosenblad, C., Kirik, D., Moffat, B., Simmons, L., Johnson, E., Jr., Milbrandt, J., Rosenthal, A., Bjorklund, A., Vandlen, R. A., Hynes, M. A., and Phillips, H. S. (1998) Neurturin exerts potent actions on survival and function of midbrain dopaminergic neurons. *J. Neurosci.* **18,** 4929–4937
18. Bonanomi, D., Chivatakarn, O., Bai, G., Abdesselem, H., Lettieri, K., Marquardt, T., Pierchala, B. A., and Pfaff, S. (2012) Ret is a multifunctional coreceptor that integrates diffusible- and contact- axon guidance signals. *Cell* **148,** 568–582
19. Shneider, N. A., Brown, M. N., Smith, C. A., Pickel, J., and Alvarez, F. J. (2009) γ Motor neurons express distinct genetic markers at birth and require muscle spindle-derived GDNF for postnatal survival. *Neural Dev.* **4,** 10.1186/1749-8104-4-42
20. Gould, T. W., Yonemura, S., Oppenheim, R. W., Ohmori, S., and Enomoto, H. (2008) The neurotrophic effects of glial cell line-derived neurotrophic factor on spinal motoneurons are restricted to fusimotor subtypes. *J. Neurosci.* **28,** 2131–2146
21. Kramer, E. R., Knott, L., Su, F., Dessaud, E., Krull, C. E., Helmbacher, F., and Klein, R. (2006) Cooperation between GDNF/Ret and ephrinA/EphA4 signals for motor-axon pathway selection in the limb. *Neuron* **50,** 35–47
22. Luo, W., Enomoto, H., Rice, F. L., Milbrandt, J., and Ginty, D. D. (2009) Molecular identification of rapidly adapting mechanoreceptors and their developmental dependence on ret signaling. *Neuron* **64,** 841–856
23. Bourane, S., Garces, A., Venteo, S., Pattyn, A., Hubert, T., Fichard, A., Puech, S., Boukhaddaoui, H., Baudet, C., Takahashi, S., Valmier, J., and Carroll, P. (2009) Low-threshold mechanoreceptor subtypes selectively express MafA and are specified by Ret signaling. *Neuron* **64,** 857–870
24. Molliver, D. C., Wright, D. E., Leitner, M. L., Parsadanian, A. S., Doster, K., Wen, D., Yan, Q., and Snider, W. D. (1997) IB4-binding DRG neurons switch from NGF to GDNF dependence in early postnatal life. *Neuron* **19,** 849–861
25. Luo, W., Wickramasinghe, S. R., Savitt, J. M., Griffin, J. W., Dawson, T. M., and Ginty, D. D. (2007) A hierarchical NGF signaling cascade controls Ret-dependent and Ret-independent events during development of nonpeptidergic DRG neurons. *Neuron* **54,** 739–754
26. Franck, M. C., Stenqvist, A., Li, L., Hao, J., Usoskin, D., Xu, X., Wiesenfeld-Hallin, Z., and Ernfors, P. (2011) Essential role of Ret for defining nonpeptidergic nociceptor phenotypes and function in the adult mouse. *Eur. J. Neurosci.* **33,** 1385–1400
27. Nishino, J., Mochida, K., Ohfuji, Y., Shimazaki, T., Meno, C., Ohishi, S., Matsuda, Y., Fujii, H., Saijoh, Y., and Hamada, H. (1999) GFR α3, a com-

ponent of the artemin receptor, is required for migration and survival of the superior cervical ganglion. *Neuron* **23,** 725–736
28. Enomoto, H., Crawford, P. A., Gorodinsky, A., Heuckeroth, R. O., Johnson, E. M., Jr., and Milbrandt, J. (2001) RET signaling is essential for migration, axonal growth and axon guidance of developing sympathetic neurons. *Development* **128,** 3963–3974
29. Honma, Y., Araki, T., Gianino, S., Bruce, A., Heuckeroth, R., Johnson, E., and Milbrandt, J. (2002) Artemin is a vascular-derived neurotrophic factor for developing sympathetic neurons. *Neuron* **35,** 267–282
30. Moore, M. W., Klein, R. D., Fariñas, I., Sauer, H., Armanini, M., Phillips, H., Reichardt, L. F., Ryan, A. M., Carver-Moore, K., and Rosenthal, A. (1996) Renal and neuronal abnormalities in mice lacking GDNF. *Nature* **382,** 76–79
31. Pichel, J. G., Shen, L., Sheng, H. Z., Granholm, A. C., Drago, J., Grinberg, A., Lee, E. J., Huang, S. P., Saarma, M., Hoffer, B. J., Sariola, H., and Westphal, H. (1996) Defects in enteric innervation and kidney development in mice lacking GDNF. *Nature* **382,** 73–76
32. Sánchez, M. P., Silos-Santiago, I., Frisén, J., He, B., Lira, S. A., and Barbacid, M. (1996) Renal agenesis and the absence of enteric neurons in mice lacking GDNF. *Nature* **382,** 70–73
33. Cacalano, G., Fariñas, I., Wang, L. C., Hagler, K., Forgie, A., Moore, M., Armanini, M., Phillips, H., Ryan, A. M., Reichardt, L. F., Hynes, M., Davies, A., and Rosenthal, A. (1998) GFR$\alpha$1 is an essential receptor component for GDNF in the developing nervous system and kidney. *Neuron* **21,** 53–62
34. Enomoto, H., Araki, T., Jackman, A., Heuckeroth, R. O., Snider, W. D., Johnson, E. M., Jr., and Milbrandt, J. (1998) GFR $\alpha$1-deficient mice have deficits in the enteric nervous system and kidneys. *Neuron* **21,** 317–324
35. Kjaer, S., Kurokawa, K., Perrinjaquet, M., Abrescia, C., and Ibáñez, C. F. (2006) Self-association of the transmembrane domain of RET underlies oncogenic activation by MEN2A mutations. *Oncogene* **25,** 7086–7095
36. Durick, K., Wu, R.-Y., Gill, G. N., and Taylor, S. S. (1996) Mitogenic signaling by Ret/ptc2 requires association with Enigma via a LIM domain. *J. Biol. Chem.* **271,** 12691–12694
37. Pandey, A., Duan, H., Di Fiore, P. P., and Dixit, V. M. (1995) The Ret receptor protein tyrosine kinase associates with the SH2-containing adapter protein Grb10. *J. Biol. Chem.* **270,** 21461–21463
38. Pandey, A., Liu, X., Dixon, J. E., Di Fiore, P. P., and Dixit, V. M. (1996) Direct association between the Ret receptor tyrosine kinase and the Src homology 2-containing adapter protein Grb7. *J. Biol. Chem.* **271,** 10607–10610
39. Iwashita, T., Asai, N., Murakami, H., Matsuyama, M., and Takahashi, M. (1996) Identification of tyrosine residues that are essential for transforming activity of the ret proto-oncogene with MEN2A or MEN2B mutation. *Oncogene* **12,** 481–487
40. Lorenzo, M. J., Gish, G. D., Houghton, C., Stonehouse, T. J., Pawson, T., Ponder, B. A., and Smith, D. P. (1997) RET alternative splicing influences the interaction of activated RET with the SH2 and PTB domains of Shc, and the SH2 domain of Grb2. *Oncogene* **14,** 763–771
41. Asai, N., Murakami, H., Iwashita, T., and Takahashi, M. (1996) A mutation at tyrosine 1062 in MEN2A-Ret and MEN2B-Ret impairs their transforming activity and association with shc adaptor proteins. *J. Biol. Chem.* **271,** 17644–17649
42. Arighi, E., Alberti, L., Torriti, F., Ghizzoni, S., Rizzetti, M. G., Pelicci, G., Pasini, B., Bongarzone, I., Piutti, C., Pierotti, M. A., and Borrello, M. G. (1997) Identification of Shc docking site on Ret tyrosine kinase. *Oncogene* **14,** 773–782
43. Grimm, J., Sachs, M., Britsch, S., Di Cesare, S., Schwarz-Romond, T., Alitalo, K., and Birchmeier, W. (2001) Novel p62dok family members, dok-4 and dok-5, are substrates of the c-Ret receptor tyrosine kinase and mediate neuronal differentiation. *J. Cell Biol.* **154,** 345–354
44. Hayashi, H., Ichihara, M., Iwashita, T., Murakami, H., Shimono, Y., Kawai, K., Kurokawa, K., Murakumo, Y., Imai, T., Funahashi, H., Nakao, A., and Takahashi, M. (2000) Characterization of intracellular signals via tyrosine 1062 in RET activated by glial cell line-derived neurotrophic factor. *Oncogene* **19,** 4469–4475
45. Kurokawa, K., Iwashita, T., Murakami, H., Hayashi, H., Kawai, K., and Takahashi, M. (2001) Identification of SNT/FRS2 docking site on RET receptor tyrosine kinase and its role for signal transduction. *Oncogene* **20,** 1929–1938
46. Melillo, R. M., Santoro, M., Ong, S. H., Billaud, M., Fusco, A., Hadari, Y. R., Schlessinger, J., and Lax, I. (2001) Docking protein FRS2 links the protein tyrosine kinase RET and its oncogenic forms with the mitogen-activated protein kinase signaling cascade. *Mol. Cell. Biol.* **21,** 4177–4187
47. Melillo, R. M., Carlomagno, F., De Vita, G., Formisano, P., Vecchio, G., Fusco, A., Billaud, M., and Santoro, M. (2001) The insulin receptor substrate (IRS)-1 recruits phosphatidylinositol 3-kinase to Ret: evidence for a competition between Shc and IRS-1 for the binding to Ret. *Oncogene* **20,** 209–218
48. Besset, V., Scott, R. P., and Ibáñez, C. F. (2000) Signaling complexes and protein-protein interactions involved in the activation of the Ras and phosphatidylinositol 3-kinase pathways by the c-Ret receptor tyrosine kinase. *J. Biol. Chem.* **275,** 39159–39166
49. Pierchala, B. A., Milbrandt, J., and Johnson, E. M., Jr. (2006) Glial cell line-derived neurotrophic factor-dependent recruitment of Ret into lipid rafts enhances signaling by partitioning Ret from proteasome-dependent degradation. *J. Neurosci.* **26,** 2777–2787
50. Pan, Q., Shai, O., Lee, L. J., Frey, B. J., and Blencowe, B. J. (2008) Deep surveying of alternative splicing complexity in the human transcriptome by high-throughput sequencing. *Nat. Genet.* **40,** 1413–1415
51. Wang, E. T., Sandberg, R., Luo, S., Khrebtukova, I., Zhang, L., Mayr, C., Kingsmore, S. F., Schroth, G. P., and Burge, C. B. (2008) Alternative isoform regulation in human tissue transcriptomes. *Nature* **456,** 470–476
52. Myers, S. M., Eng, C., Ponder, B. A., and Mulligan, L. M. (1995) Characterization of RET proto-oncogene 3′ splicing variants and polyadenylation sites: a novel C-terminus for RET. *Oncogene* **11,** 2039–2045
53. Amoresano, A., Incoronato, M., Monti, G., Pucci, P., de Franciscis, V., and Cerchia, L. (2005) Direct interactions among Ret, GDNF, and GFR$\alpha$1 molecules reveal new insights into the assembly of a functional three-protein complex. *Cell Signal.* **17,** 717–727
54. Kjaer, S., and Ibáñez, C. F. (2003) Identification of a surface for binding to the GDNF-GFR $\alpha$ 1 complex in the first cadherin-like domain of RET. *J. Biol. Chem.* **278,** 47898–47904
55. Turner, N., and Grose, R. (2010) Fibroblast growth factor signalling: from development to cancer. *Nat. Rev. Cancer* **10,** 116–129
56. Mulligan, L. (2014) RET revisited: expanding the oncogenic portfolio. *Nat. Rev. Cancer* **14,** 173–186
57. Schuchardt, A., D'Agati, V., Larsson-Blomberg, L., Costantini, F., and Pachnis, V. (1994) Defects in the kidney and enteric nervous system of mice lacking the tyrosine kinase receptor Ret. *Nature* **367,** 380–383
58. Tsui-Pierchala, B. A., Ahrens, R. C., Crowder, R. J., Milbrandt, J., and Johnson, E. M., Jr. (2002) The long and short isoforms of Ret function as independent signaling complexes. *J. Biol. Chem.* **277,** 34618–34625

# Exon Skipping in the *RET* Gene Encodes Novel Isoforms That Differentially Regulate RET Protein Signal Transduction

Nicole A. Gabreski, Janki K. Vaghasia, Silvia S. Novakova, Neil Q. McDonald and Brian A. Pierchala

*J. Biol. Chem. 2016, 291:16249-16262.*
*doi: 10.1074/jbc.M115.709675 originally published online May 23, 2016*

---